Otto et al. EPJ Techniques and Instrumentation 2014, 1:3
www.epjtechniquesandinstrumentation.com/content/1/1/3

EPJ Techniques and Instrumentation
a SpringerOpen Journal

EPJ.org

RESEARCH ARTICLE Open Access

Direct IR excitation in a fast ion beam: application to NO^- photodetachment cross sections

Rico Otto, Amelia W Ray, Jennifer S Daluz and Robert E Continetti*

* Correspondence:
rcontinetti@ucsd.edu
Department of Chemistry and Biochemistry, University of California, San Diego, 9500 Gilman Drive, La Jolla, CA, 92093–0340, USA

Abstract

Background: Optical access to a travelling ion packet is required in many ion beam experiments that study ion-photon interactions.

Methods: An approach is described for carrying out direct infrared excitation of a fast ion beam that uses an optical-quality reflective beam blocker to illuminate a counter propagating pulsed ion beam in a collinear configuration. This arrangement provides optical access along the axis of ion beam propagation by placing a mirror in the beam path at a 25 degree angle. The ion packet is bumped over the mirror, which is also used to block fast neutral particles produced during ion beam acceleration that also propagate along the beam path.

Results: The efficiency of this setup is demonstrated in a photodetachment experiment on NO^- anions, where a photoinduced depletion of up to 90% of the beam is achieved in a single laser shot. To demonstrate the application of this configuration, the relative photodetachment cross section for NO^- has been measured in the range of 2800 – 7200 cm-1. The measured relative cross section shows a set of sharp peaks that are identified as vibrational autodetachment resonances.

Conclusion: The new setup paves the way for future experiments where parent anionic species are vibrationally excited via direct infrared excitation first and undergo photodetachment/photodissociation in a subsequent step.

Keywords: Infrared excitation; Fast ion beam; Nitric oxide anion photodetachment

PACS: 33.15.Ry; 33.80.Eh; 33.80.-b

Background

Optical access to a travelling ion packet is required in many ion beam experiments that study ion-photon interactions. Ion storage rings can provide optical access tangentially to the beam path, thereby enabling lifetime measurements of metastable ions [1]. Multipass cell [2,3] or resonator [4] arrangements are used to increase the overlap between a short laser pulse and a molecular beam. Developments in manufacturing microchannel plate (MCP) ion detectors have enabled photofragmentation experiments where a detector featuring a center hole allows laser access to a fast moving ion packet [5]. Cluster predissociation studies often make use of a spatial and temporal focus of the ion bunch to maximize the overlap with a laser that crosses the beam from the side [6]. However, due to conservation of phase space, such a focus will always create an axial energy spread of the beam that might be undesirable if the kinetic energy release of the fragments is of interest. The work presented here was inspired by the need to

illuminate an outstretched ion packet (~30 cm) in a completely collinear ion beam experiment, in which photoelectrons and photofragments created from a fast moving ion beam are collected in coincidence (PPC) [7].

The fast-beam apparatus used in these studies features a plasma discharge ion source where anions are created in a supersonic expansion at a 10 Hz duty cycle. The ions pass through a skimmer together with the gas jet and can be accelerated up to 10 keV, with an energy spread of less than 0.1 eV, before being re-referenced to ground while traveling through a cylindrical electrode. The length of this cylinder (30 cm) determines the spatial extension of the ion packet. After a flight distance of ~1 m the ion packet is injected into an electrostatic ion trap (EIBT), where it is repetitively probed perpendicularly with the pulsed output from a 1 kHz Ti:Sapphire laser system for studies of photodetachment and dissociative photodetachment processes. As part of an effort to expand the present set of experiments towards direct infrared excitation of the parent anionic species prior to the photodetachment step, it has become essential to irradiate the entire outstretched ion packet with the output of a 10 Hz infrared (IR) optical parametric oscillator/optical parametric amplifier (OPO/OPA) laser system before it enters the EIBT. In addition, such an arrangement opens up the possibility to study photodetachment processes in weakly bound anionic species.

Here we demonstrate a simple configuration where a single gold mirror is placed in the ion beam, with the surface normal of the mirror at an angle of 25 degrees relative to the ion beam propagation direction. The pulsed IR laser light enters the vacuum through a viewport located on the side of the vacuum chamber such that it forms an angle of 50 degrees with the beam axis. The laser pulse reflects off the gold mirror and illuminates the entire ion bunch in a single shot. The ions are then electrostatically bumped over the mirror and corrected to the ion beam axis to continue travelling towards the EIBT. As a secondary effect, the gold mirror acts as a beam blocker for fast neutral particles in the beam, preventing this source of background from striking the neutral particle detector used in the PPC experiments. This also ensures ultra-high vacuum conditions in the EIBT and detection regions. The performance of the new setup was demonstrated in a photodetachment experiment, making use of the small electron affinity (EA = 26 ± 5 meV) [8] of the NO molecule to directly deplete ions from a fast ion beam. A measurement of the wavelength dependence of the depletion, which is proportional to the photodetachment cross section, reveals sharp resonance features that are associated with vibrational transitions in the NO^- anion, followed by vibrational autodetachment.

Results and discussion

Design and performance of the reflective beam blocker

Depicted in Figure 1 is the reflective beam blocker design, consisting of a rectangular gold mirror (3 × 1 cm) that is attached to an L-bracket aluminum holder. The assembly is located in an electrode arrangement that bumps the ion packet over the mirror and returns it to the incident beam axis. To ensure good electrical conductivity with the mirror's surface, the edges of the mirror were connected to the aluminum substrate using a colloidal silver paint. For practical reasons the mirror is placed in the beam centerline at an angle of 25 degrees, allowing for coupling in an IR laser beam through

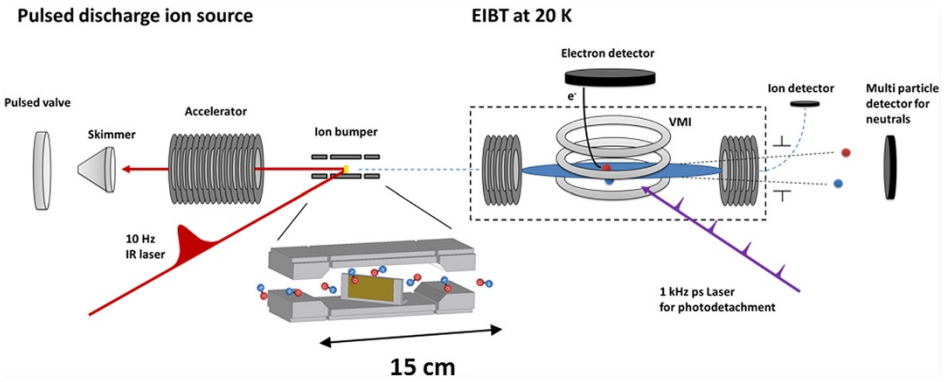

Figure 1 Schematic of the reflective beam blocker setup. Ions are produced in a pulsed discharge and accelerated to 7 keV. A gold mirror is placed in the beam path to illuminate the fast moving ion packet with a 10 Hz IR laser pulse. A set of electrostatic electrodes is used to bump the ion beam over the reflective beam blocker. On the way to the ion detector the ion beam enters an electrostatic ion beam trap (EIBT) dedicated to photoelectron-photofragment coincidence (PPC) experiments.

a CaF vacuum viewport located on the side of the ion-beam transport chamber. The ion deflection unit consists of three sets of electrostatic electrodes that are used to transfer the ion packet over the mirror before returning it to the original trajectory. The first and last deflector electrodes are held at identical potentials (V1, V3) while the electric field is reversed for the center deflector (V2). The voltages for all deflectors are in the range of 700 – 850 V, with typical values for V1 and V3 of about $0.9 \cdot V2$. The voltages that need to be employed in order to effectively transfer the ion packet over the mirror were optimized using SIMION [9]. In addition to its vertical deflection properties, the simulations revealed a small focusing effect on the vertical axis of the ion deflector unit. In the experiment this effect is accounted for with an additional set of ion optics after the unit. Further details of the experimental approach are provided in the Methods section below.

Figure 2 shows the depletion N_{IR}/N_0 as a function of the temporal delay of the incoming IR pulse with respect to the ion source, measured at an IR wavelength of

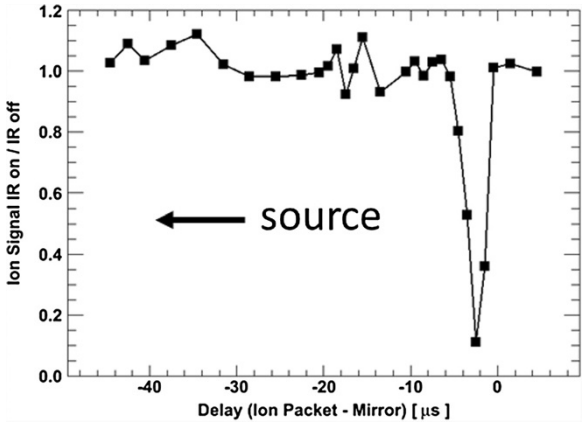

Figure 2 Depletion of an NO^- ion beam (N_{IR}/N_0) due to interaction with a single infrared laser pulse. The data shows the photodetachment induced depletion as a function of probing the ion packet at different distances from the mirror towards the ion source (negative delays). The best beam overlap is achieved in the region close to the mirror, where a maximum depletion of 90% is demonstrated in a single shot.

5300 cm^{-1}. Changing this delay probes the ion packet at different positions along the beam axis, where a delay of 0 μs corresponds to a laser pulse entering the chamber as the ion packet travels over the mirror, while at earlier timings the packet is still closer to the ion source. A maximum in the depletion is achieved shortly before the ion packet is transferred over the mirror. This can be attributed to the shape and trajectory of the travelling ion packet, which is collimated using an Einzel lens before approaching the mirror. The measured depletion gives an upper limit to the fraction of ions detached in a single laser shot of 90%. Note that this result also provides a lower limit to the fraction of ions that are illuminated, regardless of the laser power.

The depletion measurements outlined above can be used to measure the relative photodetachment cross section of the NO^- molecule. In general the ion-laser interaction leads to an exponential decay of the signal N_0 so that the signal after a short laser pulse of temporal length t can be written as

$$N(t) = N_0 \cdot \exp(-kt) \tag{1}$$

with a photodetachment-induced decay rate k that can be expressed as

$$k = F_L \cdot \sigma \cdot \rho. \tag{2}$$

This decay rate depends only on the total photon flux F_L (cm^{-2} s^{-1}), the photodetachment cross section σ (Mbarn = 10^{-18} cm^2) and the geometrical overlap ρ between the ion packet and the laser beam. While the geometrical overlap and the exact beam profile of the laser in the chamber are unknown, it is assumed that they remain constant within ± 20% over the course of the experiment, as inferred by projecting the IR beam in the far field. An upper limit for the laser beam diameter is given by the apertures of about 1 cm in the ion time-of-flight region. In order to determine the total photon flux F_L the power P_{IR} at each wavelength was measured at the output port of the IR laser using a power meter (Ophir Nova). The IR wavelength λ was determined via the OPO signal and idler wavelength using a spectrometer (Ocean Optics HR2000+) and independently calibrated using a photo acoustic spectroscopy setup. Furthermore, the fast moving ion packet gives rise to a Doppler shift of the counter propagating IR pulse, which accounts for 2 – 5 cm^{-1} over the range of the experiment and has been corrected for. The Doppler spread due to the axial energy uncertainty of the ion beam is in the range of a few MHz and is therefore much smaller than the bandwidth of the pulsed IR laser system. The laser beam had to undergo reflections from a total of six gold mirrors and cross a CaF vacuum window before counter propagating into the ion beam. The reflectivity for the mirrors (98 ± 0.5%) as well as the transmittance of the CaF window (94 ± 0.5%) can be considered constant over the measured wavelength range, so that the measured laser power multiplied by the photon wavelength is proportional to the photon flux in the ion interaction region. A relative photodetachment cross section is then given by

$$\sigma_{PD} \propto -\log(N_{IR}/N_0)/(P_{IR} \cdot \lambda). \tag{3}$$

Shown in Figure 3 is the relative photodetachment cross section measured as a function of the photon energy in the range 2800 – 7200 cm^{-1}. These data represent the average of a large number of datasets that have been concatenated such that

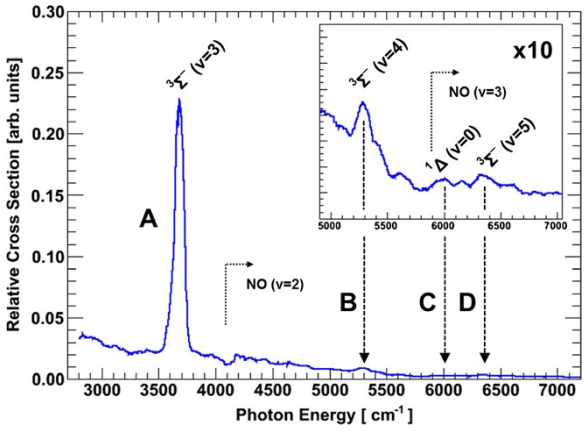

Figure 3 NO^- photodetachment relative cross section measured in the range 2800 – 7200 cm^{-1}. The observed peaks are assigned to vibrational autodetachment resonances NO^- (v = 0) → NO^- (v′ > 0). At 4090 cm^{-1} and 5903 cm^{-1} the thresholds for the NO^- (v = 0) → NO (v = 2) and NO^- (v = 0) → NO (v = 3) direct photodetachment are observed.

overlapping frequency ranges match up. For these measurements the optimum temporal delay, derived from Figure 2, has been used.

The shape of the cross section makes it obvious that two different processes are observed in the experiment. The first process is a bound-free transition between the molecular anion and a neutral NO molecule plus an electron in the continuum. This process is responsible for the continuous part of the spectrum that slowly decreases with increasing photon energy. On top of that resonant peaks are observed that are identified as vibrational transitions induced in the NO^- molecule by IR absorption, followed by autodetachment.

Direct photodetachment of NO^-

Molecular photodetachment has been shown to provide a sensitive tool to probe both the initial anion [10] and final neutral state [11]. According to Wigner's law the energy dependence of the cross section close to threshold scales as

$$\sigma(E) \propto (E - E_0)^{2l+1} \tag{4}$$

with the threshold energy E_0 and the angular momentum l of the outgoing electron. The more complex zero core contribution (ZCC) model [12] has been used to describe the shape of the cross section above threshold for atomic systems. While the Wigner law is well suited to describe the rising cross section behavior close to the threshold, the ZCC model also reproduces a decaying cross section at higher energies. Al-Za'al *et al.* applied the model to NO^- photodetachment and predicted a sharp rise in the cross section at 0.507 eV (4090 cm^{-1}), which is associated with the channel to produce NO (v = 2) opening up [13]. Surprisingly they could not verify this threshold experimentally. Instead a continuous spectrum without sharp increases was observed that slowly decreased over the experimental range. The authors based their analysis on the electron affinity for the NO^- (v = 0) → NO (v = 2) transition measured by Siegel *et al.* [14], and added a rotational correction of 12.5 meV. Based on those values another rise in the cross section is expected at 0.732 eV (5903 cm^{-1}) where the NO (v = 3) state becomes accessible. More recent photoelectron spectroscopy experiments suggest values

of 0.488 eV and 0.714 eV for the NO (v = 2) and NO (v = 3) electron affinity relative to NO^- (v = 0) [8].

In the results reported here a slowly decaying cross section attributed to direct photodetachment that is accompanied by several sharp resonance features is observed. The continuous part of the cross section decays by a factor of 10 over the measured range. Upon closer inspection, two regions in the spectrum at 4100 cm^{-1} and 5900 cm^{-1} can be identified where a sudden increase in the cross section is observed. Both of these features are assigned to the opening of new product channels, leading to NO (v = 2) and NO (v = 3) products respectively, as indicated in the figure. The cross section at the (v = 2) threshold rises by almost a factor of two, in accordance with the predictions from the ZCC model [13]. It is interesting to note that above this threshold the cross section reaches a maximum after only 100 cm^{-1} before starting to decrease again. The (v = 3) threshold is not analyzed here, since it is located close to one of the resonance features that will be discussed in the next section.

Photoinduced Vibrational Autodetachment of NO^-

Two previous studies have examined photodetachment of NO^- in the IR [13,15]. Maricq *et al.* used diode lasers to study the photodetachment cross section in the range 1100 – 1500 cm^{-1}. To cover the frequency range of the experiment three different diode lasers were used that had line widths between 1 and 10 cm^{-1}. They found a vibrational autodetachment resonance centered at 1284 cm^{-1} assigned to the NO^- (v = 0) → NO^- (v = 1) transition and reported a width of the observed resonance of 95 cm^{-1}, attributed to lifetime broadening. Al-Za'al *et al.* studied the NO^- cross section in the range 3000 – 4150 cm^{-1} using an F-center laser. They reported a continuous spectrum without any evidence for vibrational resonances. The observed monotonic decrease of 50% over the measured range was interpreted as the high energy tail of the NO^- (v = 0) → NO^- (v = 2) vibrational resonance. This scenario, however, requires the resonance to have a width of 600 cm^{-1} that seems unlikely. Prior data from photodetachment studies is scarce but vibrational autodetachment resonances have been studied in numerous electron scattering experiments [14,16-19] arising from electron attachment to NO(v = 0) forming an intermediate NO^-(v' > 0) excited state. The energy of the electron beam is thereby given relative to the ground state of NO. Therefore, in order to compare these values to a photodetachment experiment it is essential to take into account the electron affinity of the NO molecule, measured to be 26 meV in previous photodetachment experiments [8]. The variation among these earlier experiments is summarized in Figure 4 for the NO^- resonances associated with the vibrational levels (v = 1 – 5) of the NO^- $^3\Sigma^-$ state.

The data presented in this work shows a series of distinct resonant peaks in the photodetachment cross section (see Figure 3). The positions of the peaks labeled A – D are listed in Table 1. Based on the comparison with the electron scattering data, the peaks A and B are assigned to the vibrational transitions NO^- (v = 0) → NO^- (v = 3, 4) within the $^3\Sigma^-$ anion ground state. In previous experimental studies by Tronc *et al.* [19] the width of the NO^- (v = 5) resonance was observed to be much broader than the NO^- (v = 1 – 4) series, which was attributed to a superposition of the NO^- ($^3\Sigma^-$, v = 5) and NO^- ($^1\Delta$, v = 0) state. Ziesel *et al.* [17] resolved the splitting caused by the two states more clearly, but observed a line shape that required a superposition of three peaks to

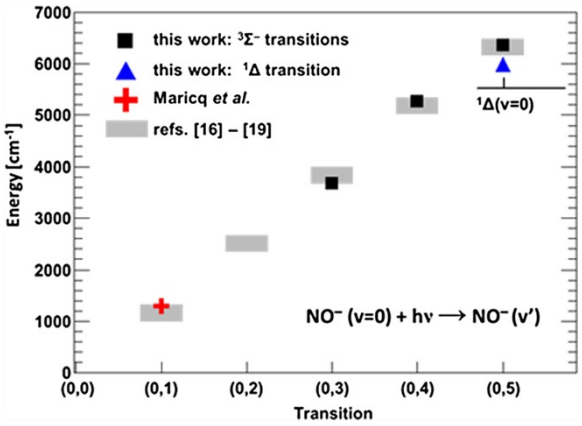

Figure 4 Energy of the vibrational resonances in NO^- recorded in previous studies and this work. The data from electron scattering experiments (range given by grey boxes) have been shifted by 26 meV to be directly comparable to values from photodetachment studies (markers) including the results of Maricq *et al.* reported in ref. 15. The position of the $NO^-(^3\Sigma^-, v = 0) \rightarrow NO^-(^1\Delta, v = 0)$ transition is shown on the inset axis.

achieve the best fit to their data. Based on these previous studies, peaks C and D are assigned to the NO^- ($^1\Delta$, v = 0) and NO^- ($^3\Sigma^-$, v = 5) resonances, respectively. A comparison of this new photodetachment data with the range of previous measurements is shown in Figure 4, where it is seen that the positions of the peaks observed are well within the range of previously measured resonance features.

The observed intensity of the resonance peaks is largest for the (v = 3) resonance and decreases for higher vibrational excitation, which can be understood in terms of a decreasing Franck-Condon overlap [20]. The fact that the NO^- (v = 3) level is nearly degenerate with NO (v = 2) also contributes to the high intensity of the (v = 3) resonance. Finally, it is interesting to note that the spacing found between the (v = 3) and (v = 4) resonances is significantly larger ($\Delta E = 1600\ cm^{-1}$) than that between the (v = 4) and (v = 5) feature ($\Delta E = 1100\ cm^{-1}$). The resonance features detected in electron scattering show a consistent spacing of about 0.16 eV ($1300\ cm^{-1}$) at least up to (v = 9), pointing to only weak anharmonicity in the NO^- potential. However, it has to be pointed out that the underlying mechanism in those experiments is different in nature than the direct bound-bound transition probed in vibrational autodetachment. Also, it cannot be ruled out that rotational effects might play an important role in the autodetachment process [21]. An analysis of such effect is beyond the scope of this work.

Conclusions

A new experimental setup has been presented here that allows direct IR excitation in a completely collinear pulsed ion beam experiment that does not feature any other

Table 1 Peak positions observed in the photodetachment cross section of NO^-

Peak	Energy (cm^{-1})	Width (cm^{-1})	Assignment
Ref. ([15])	1284 ± 10	95 ± 15	$^3\Sigma^-$ (v = 1)
A	3687 ± 2	28 ± 3	$^3\Sigma^-$ (v = 3)
B	5290 ± 3	41 ± 3	$^3\Sigma^-$ (v = 4)
C	5976 ± 13	108 ± 24	$^1\Delta$ (v = 0)
D	6355 ± 10	115 ± 16	$^3\Sigma^-$ (v = 5)

optical access along the ion beam path. This has been achieved by placing an optical-quality mirror in the beam path at an angle that allows coupling in an IR laser from the side of the setup. Photodetachment-induced depletion of an NO^- beam was used to demonstrate the overlap that can be achieved between the laser pulses and a fast moving ion packet. Furthermore, measurements of the relative photodetachment cross section of the NO^- molecule in the range of 2800 – 7200 cm^{-1} were made. It was found that the cross section in this range is a combination of direct photodetachment and vibrational autodetachment. The observed autodetachment resonances are within the range of previous experimental results from electron scattering experiments.

This new setup paves the way for future PPC studies with vibrationally excited molecules. In these experiments molecular anions will be prepared in specific vibrational states before entering the ion beam trap, and the fragmentation dynamics in dissociative photodetachment processes will be studied. The systems amenable to study by this approach will in general be strongly bound anions where the lifetimes of the excited vibrational modes are long enough to allow for transferring the ions over the mirror and carrying out PPC experiments on a millisecond timescale.

Methods

To demonstrate the capabilities of the reflective beam blocker design for coupling a light source with a travelling ion packet, a photodetachment experiment using a beam of NO^- molecules was carried out. These experiments exploit the low electron affinity of NO^- that allows for efficient photodetachment at wavelengths between 2 – 5 μm. The NO^- anions were generated from a 10 Hz pulsed discharge (20% N_2O seeded in a 1:2 He/Ne mixture, 20 psi stagnation pressure). Typical rotational temperatures for this ion source have been measured to be 50 – 100 K using near threshold photodetachment of OH^- in a different set of experiments. The ions were accelerated to 7 keV before approaching the reflective beam blocker. The ion signal was monitored 2.5 m behind the beam blocker using an off-axis MCP ion detector. Tunable IR laser pulses from a 10 Hz Nd:YAG (Surelite III EX) pumped OPO/OPA system (LaserVision, 5 ns FWHM, 3 cm^{-1} bandwidth) were coupled into the approaching ion packet at a time delay synchronized with the pulsed ion source. A typical output power between 100 and 300 mW can be achieved over the wavelength range covered in this work. The depletion of the beam caused by photodetachment of the NO^- was derived from consecutively measuring the IR on and IR off ion signals (denoted as N_{IR} and N_0 respectively) at a given wavelength. To acquire each signal an average over 32 source cycles was recorded before the status of the IR laser was switched (IR on/off).

Abbreviations

MCP: Microchannel plate; PPC: Photoelectron photofragment coincidence; EIBT: Electrostatic ion beam trap; IR: Infrared; ZCC: Zero core contribution.

Competing interests

The authors declare that they have no competing interests.

Authors' contributions

RO designed the apparatus, carried out the experiments and drafted the manuscript. AR participated in the experiments. JD participated in the experiments and the wavelength calibration measurements. AR and JD both participated in manuscript preparation. RC conceived of the study, participated in design and coordination and helped draft the manuscript. All authors read and approved the final manuscript.

Acknowledgements
This work was supported by the U.S. Department of Energy under grant number DE-FG03-98ER14879. RO thanks the German Academic Exchange Service (DAAD) for a postdoctoral research fellowship. AWR and JSD acknowledge support from GAANN grant P200A120223 from the U.S. Dept. of Education.

Received: 5 December 2013 Accepted: 5 March 2014
Published: 29 April 2014

References

1. Andersen JU, Hvelplund P, Nielsen SB, Tomita S, Wahlgreen H, Møller SP, Pedersen UV, Forster JS, Jørgensen TJD: **The combination of an electrospray ion source and an electrostatic storage ring for lifetime and spectroscopy experiments on biomolecules.** *Rev Sci Instrum* 2002, **73:**1284–1287.
2. Gough TE, Gravel D, Miller RE: **Multiple crossing devices for laser-molecular beam spectroscopy.** *Rev Sci Instrum* 1981, **52:**802.
3. Lethbridge PG, Stace AJ: **Design considerations for the construction of a reflecting symmetric multipass cell for use in laser molecular-beam experiments.** *Rev Sci Instrum* 1987, **58:**2238–2243.
4. Hlavenka P, Plašil R, Bánó G, Korolov I, Gerlich D, Ramanlal J, Tennyson J, Glosík J: **Near infrared second overtone cw-cavity ringdown spectroscopy of D_2H^+ ions.** *Int J Mass Spectrom* 2006, **255:**170–176.
5. Toker Y, Aviv O, Eritt M, Rappaport ML, Heber O, Schwalm D, Zajfman D: **Radiative cooling of Al_4^- clusters.** *Phys Rev A* 2007, **76:**053201.
6. Ayotte P, Johnson MA: **Electronic absorption spectra of size-selected hydrated electron clusters: $(H_2O)_n^-$, n = 6–50.** *J Chem Phys* 1997, **106:**811.
7. Johnson CJ, Shen BB, Poad BLJ, Continetti RE: **Photoelectron-photofragment coincidence spectroscopy in a cryogenically cooled linear electrostatic ion beam trap.** *Rev Sci Instrum* 2011, **82:**105105.
8. Travers MJ, Cowles DC, Ellison GB: **Reinvestigation of the electron affinities of O_2 and NO.** *Chem Phys Lett* 1989, **164:**449–455.
9. Dahl DA: **SIMION 3D, Version 7.0 User's Manual INEEL-95/0403**. In *Idaho National Engineering and Environmental Laboratory, Bechtel BWXT Idaho, LLC.* 2000.
10. Otto R, von Zastrow A, Best T, Wester R: **Internal state thermometry of cold trapped molecular anions.** *Phys Chem Chem Phys* 2013, **15:**612–618.
11. Schulz PA, Mead RD, Jones PL, Lineberger WC: **OH and OD threshold photodetachment.** *J Chem Phys* 1982, **77:**1153.
12. Stehman RM, Woo SB: **Zero-core-contribution model and its application to photodetachment of atomic negative ions.** *Phys Rev A* 1979, **20:**281.
13. Al-Za'al M, Miller HC, Farley JW: **Measurement of the infrared photodetachment cross section of NO^-.** *Phys Rev A* 1986, **33:**977.
14. Siegel MW, Celotta RJ, Hall JL, Levine J, Bennett RA: **Molecular Photodetachment Spectrometry. I. The Electron Affinity of Nitric Oxide and the Molecular Constants of NO^-.** *Phys Rev A* 1972, **6:**607.
15. Maricq MM, Tanguay NA, O'Brien JC, Rodday SM, Rinden E: **Vibrational autodetachment of NO^-.** *J Chem Phys* 1989, **90:**3136.
16. Spence D, Schulz GJ: **Vibrational Excitation and Compound States in NO.** *Phys Rev A* 1968, **1971:**3.
17. Randell J, Lunt SL, Mrotzek G, Field D, Ziesel JP: **Low-energy negative-ion states of NO at high electron energy resolution.** *Chem Phys Lett* 1996, **252:**253–257.
18. Alle DT, Brennan MJ, Buckman SJ: **Low-energy total electron scattering cross section and electron affinity for NO.** *J Phys B Atomic Mol Phys* 1996, **29:**L277.
19. Tronc M, Huetz A, Landau M, Pichou F, Reinhardt J: **Resonant vibrational excitation of the NO ground state by electron impact in the 0.1–3 eV energy range.** *J Phy B* 1975, **8:**1160.
20. Teillet-Billy D, Fiquet-Fayard F: **The NO^- $^3\Sigma^-$ and $^1\Delta$ resonances: theoretical analysis of electron scattering data.** *J Phy B* 1977, **10:**L111.
21. Neumark DM, Lykke KR, Andersen T, Lineberger WC: **Infrared spectrum and autodetachment dynamics of NH^-.** *J Chem Phys* 1985, **83:**4364.

doi:10.1140/epjti3
Cite this article as: Otto *et al.*: Direct IR excitation in a fast ion beam: application to NO^- photodetachment cross sections. *EPJ Techniques and Instrumentation* 2014 **1**:3.